

Method of analytical regularization based on the static part inversion in wave scattering by imperfect thin screens

Alexander I. Nosich

Abstract — The paper is focussed on the development of the method of analytical regularization (MAR) in electromagnetic wave scattering and absorption by imperfect scatterers shaped as thin screens.

Keywords — wave scattering, imperfect boundary conditions, thin screens, regularization.

1. Imperfect boundary conditions

As known (see [1–6]), if the thickness of imperfect scatterer is small compared to the free-space wavelength, the wave scattering problem can be simplified to exclude the internal field from consideration. This is done by assuming the scatterer thickness to be zero but at the same time introducing specific boundary conditions modified with respect to the perfectly electric conducting (PEC) boundary conditions. In these conditions, certain effective parameters appear, accumulating the values of the thickness and material constants of the scatterer. These parameters couple together the limit values of the tangential field components \vec{E}_T^\pm and \vec{H}_T^\pm on the two sides of the scatterer, namely, their jumps and their mean values. In all, there are three different conditions of this type [4]:

1) resistive:

$$\frac{1}{2}[\vec{E}_T^+ + \vec{E}_T^-] = Z_0 R \vec{n} \times [\vec{H}_T^+ - \vec{H}_T^-], \quad (1)$$

$$\vec{E}_T^+ = \vec{E}_T^-, \quad (2)$$

2) material, or magneto-dielectric:

$$\frac{1}{2}[\vec{E}_T^+ + \vec{E}_T^-] = Z_0 R \vec{n} \times [\vec{H}_T^+ - \vec{H}_T^-], \quad (3)$$

$$\frac{1}{2}[\vec{H}_T^+ + \vec{H}_T^-] = -\frac{S}{Z_0} \vec{n} \times [\vec{E}_T^+ - \vec{E}_T^-], \quad (4)$$

and

3) impedance one:

$$\frac{1}{2}[\vec{E}_T^+ + \vec{E}_T^-] = Z_0 R \vec{n} \times [\vec{H}_T^+ - \vec{H}_T^-] + W[\vec{E}_T^+ - \vec{E}_T^-], \quad (5)$$

$$\frac{1}{2}[\vec{H}_T^+ + \vec{H}_T^-] = -\frac{S}{Z_0} \vec{n} \times [\vec{E}_T^+ - \vec{E}_T^-] - W[\vec{H}_T^+ - \vec{H}_T^-]. \quad (6)$$

The first condition appears in the case of a thinner-than-skindepth metal scatterer of finite conductivity; the second one is derived for a thin magneto-dielectric scatterer (material), and the third one for a PEC scatterer covered with a thin material layer. Thin scatterers are commonly called screens and can be flat or curved. Of the three mentioned types of screens, the first two (resistive and material) are partially transparent while the third one (impedance) is non-transparent. Note that conditions (5) and (6) are of the most general form, and the first two ones can be viewed as particular cases of that form.

So, any mentioned type of thin scatterers can be simulated by using at most three effective parameters. There exists an ambiguous terminology about these parameters. We shall use the one proposed in [4] and call them resistivities: electric R , magnetic S , and so-called cross-resistivity W . For example, in the case of a thinner-than-skindepth metal sheet and a thin low-contrast dielectric sheet having normalized material parameters ϵ_r and μ_r , respectively [2, 4, 5]:

$$R_m = (Z_0 b \sigma)^{-1}, \quad R_d = i[k_0 b (\epsilon_r - 1)]^{-1} \quad (7)$$

while $S = i\infty$ and $W = 0$. Here b is the thickness, σ is the conductivity, Z_0 is the free-space impedance, k_0 is the free-space wavenumber, and it is assumed that $\mu_r = 1$, $|\epsilon_r - 1| \ll 1$ and $k_0 b \ll 1$. In the case of a thin single-layer high-contrast material sheet, it can be shown (see [1, 3, 4]) that

$$R = Z^2 S = \frac{i}{2} Z \cot \left(\frac{1}{2} \epsilon_r^{1/2} \mu_r^{1/2} k_0 b \right), \quad W = 0, \quad (8)$$

where $Z = (\mu_r / \epsilon_r)^{1/2}$, and it is assumed that $|\epsilon_r \mu_r| \gg 1$ and $k_0 b \ll 1$. Note that for a multi-layer sandwich-like material sheet, $W \neq 0$ [4].

It is interesting to recall that the conditions (1), (2) and (3), (4) were at first proposed empirically. They had been in extensive use for quite a long time (e.g., see [7–10]) before being fully grounded in [2] and [3], respectively. Mathematically rigorous derivation of the expressions (7) and (8) for the resistivities was also done in [2, 3] and confirmed more relaxed derivations of [1, 4–6].

For the sake of completeness, it should be mentioned that material screens have been also simulated by introduc-

ing the so-called “higher-order” imperfect boundary conditions [5]. The latter involve not only the limit values of tangential fields but also their normal derivatives. For example, condition (4) is modified to take the following “first-order” form (see [11]):

$$\frac{1}{2}[\vec{H}_T^+ + \vec{H}_T^-] = -\frac{1}{Z_0}\vec{n} \times \left(S - \frac{\partial}{k_0 \partial n} \right) [\vec{E}_T^+ - \vec{E}_T^-]. \quad (9)$$

In this paper, we shall base our considerations on the “zeroth-order” boundary conditions (1) – (6) although one can extend MAR to the conditions of [11]. Note that conditions of the order higher than 1 are ambiguous from the viewpoint of the solution uniqueness [12]. Further, although conditions (1) – (6) are derived for infinite thin sheets, we shall apply them to the limited screens like strips and disks, which have sharp edges. We shall not discuss here the validity of the modified conditions near the edges, and only remark that, according to [2], this is less ambiguous than using together the PEC conditions and the zero thickness of a screen with edges. Instead, we shall imply that each time some appropriate edge condition is included in the problem formulation, that guarantees the solution uniqueness.

Impenetrable thin imperfect screen is a special case when three resistivities are not independent. As shown in [4], they should satisfy the relationship

$$4(RS + W^2) = 1. \quad (10)$$

Therefore, in this case one of three resistivities can be eliminated, and the pair of conditions (5) and (6) can be equivalently formulated in terms of two other effective parameters: surface impedances Z^+ and Z^- , i.e., as the two-side Leontovich boundary conditions [4 – 6]:

$$\vec{E}_T^\pm \mp Z_0 Z^\pm \vec{n} \times \vec{H}_T^\pm = 0. \quad (11)$$

Equations (11) are equivalent to (5) and (6) provided that

$$R = \frac{Z^+ Z^-}{Z^+ + Z^-}, \quad S = \frac{1}{Z^+ + Z^-}, \quad W = \frac{1}{2} \frac{Z^+ - Z^-}{Z^+ + Z^-}, \quad Z^+ + Z^- \neq 0. \quad (12)$$

For example, a thin PEC screen coated with different layers of magneto-dielectrics of parameters b^\pm , ϵ_r^\pm and μ_r^\pm , has the values of the surface impedances given by [4 – 6]

$$Z^\pm = -iZ \tan[(\epsilon_r^\pm \mu_r^\pm)^{1/2} k_0 b^\pm]. \quad (13)$$

It is important to note that if any material parameter of an imperfect screen is not real but complex-valued, then the resistivities obtain non-zero real parts, which are responsible for the dissipation losses. Therefore, by modifying the boundary conditions, one can study not only the wave scattering but also the wave absorption. Besides, if any of the quantities ϵ_r , μ_r or h varies along the screen surface, then the resistivities R, S, W are the functions of coordinates.

2. About the method of analytical regularization

Hence, there arises a challenge to extend or modify the previously existed analytical and numerical solutions of the PEC-screen wave scattering problems to the three mentioned types of imperfect thin screens. In computational electromagnetics, one of the most powerful and efficient approaches is based on the integral equations (IE) – see [13]. Here, the method of analytical regularization, i.e., a semi-inversion of the full-wave singular IE [14], is the one that guarantees numerical convergence. General scheme of MAR works as follows. Commonly, the boundary PEC conditions generate a singular IE of the first kind: $\hat{G}X = F$. Split the operator \hat{G} into two parts, \hat{G}_1 and \hat{G}_2 . Provided that the former has a known inverse \hat{G}_1^{-1} , the original equation can be converted to the second-kind one: $X + \hat{A}X = B$, where $\hat{A} = \hat{G}_1^{-1} \hat{G}_2$ and $B = \hat{G}_1^{-1} F$. However, this scheme is mathematically justified only if the operator \hat{A} is compact, i.e., its norm $\|\hat{A}\| < \infty$ in the functional space L_2 . This implies inherently that the inverted operator \hat{G}_1 must be a singular one while \hat{G}_2 is regular. It is possible to point out several different ways of extracting out an invertible singular part of original equation. It corresponds to either canonical-shape or to the high-frequency or to the static part of the full-wave IE operator [14]. Once this has been done, it is guaranteed, thanks to the Fredholm theorems, that the usual discretization schemes converge to the exact solution in the point-wise sense. Here, the convergence is understood as a possibility to minimize the computation error to machine precision by solving progressively larger matrices.

The variety of problems solved by MAR with the static part inversion covers a wide class of PEC zero-thickness screens [14]. Among them there are single strips and strip gratings, strip irises in a waveguide, periodic circular waveguides, open circular cylindrical screens and collections of them, longitudinally slitted infinite cone, circular disk, spherical cap, finite circular hollow pipe, etc. Any of the listed problems is reduced first to a single singular IE or a coupled pair of IEs of the first kind. A limit form of IE, corresponding to the static problem, can be inverted analytically based on the theory of the Cauchy integrals. Application of this result to the full-wave IE leads to an IE of the Fredholm 2nd kind with a smooth kernel. Hence, the existence of the unique solution is guaranteed. Numerical solution is then easy to obtain by using any reasonable discretization scheme, and the validity of the matrix truncation is justified.

Discretization and partial inversion can be joined together in a single procedure, if one uses the set of orthogonal eigenfunctions of the static part of the full-wave operator as a projection basis in a Galerkin scheme [14]. As the accuracy of computations is improved by increasing the number of equations and is limited only by the digital precision of computer used, MAR may be called a “numerically exact” approach. The number of equations needed for a practi-

cal accuracy of 3–4 digits is normally slightly greater than electrical size of a PEC scatterer. As we shall see, in the 2D case of the H-polarization, these solutions can be directly extended to resistive scatterers as well, because non-zero R does not change the static limit of IE. In the E-polarization case, the situation is different. Here, non-zero R changes the static behavior of the scatterer. However, in the E-case, second-kind IE obtained from the imperfect boundary condition is already a Fredholm one, whose operator vanishes in the static limit. For the axisymmetric 3D screens, the same is valid with respect to IEs for two potential functions, which are frequently taken as E_ϕ and H_ϕ . In each case, the obtained second-kind equations correspond to the static-part inversion. It is also necessary to note that if there exists a one-to-one mapping $X = CZ$, $Z = C^{-1}X$, then one can build a MAR analysis on the discretization of the equivalent operator equation $Z + (C^{-1}AC)Z = C^{-1}B$, which is also a Fredholm second-kind one. For example, operators C and C^{-1} can be direct and inverse integral Fourier transforms (in the single strip scattering) or discrete Fourier transforms (in the strip grating scattering) or integral Hankel transforms (in the disk scattering).

3. Resistive strip scattering

Consider an example in 2D: the scattering of a given time-harmonic ($\sim e^{-i\omega t}$) electromagnetic field by a resistive strip [9, 15, 16], whose contour of cross-section is an open curve M in the plane (x, y) . Here, two alternative polarization cases can be treated separately. Generally, the scattered field has to satisfy the Helmholtz equation off M , boundary conditions on M , edge condition near the sharp edges of the screen, and the radiation condition at infinity. In the case of the H-polarization, the role of potential function is played by the magnetic-field component parallel to the strip generatrix, $H = H_z$. Then, the boundary conditions (1), (2) take the form as

$$\frac{1}{2} \left(\frac{\partial H^+}{\partial n} + \frac{\partial H^-}{\partial n} \right) + ik_0 Z_0 R (H^+ - H^-) = 0, \quad (14)$$

$$\partial H^+ / \partial n - \partial H^- / \partial n = 0. \quad (15)$$

After decomposing the total field into the sum of the incident H^{in} and scattered one H^{sc} and presenting the latter in the form of a double-layer potential, one obtains a hyper-singular integral equation of the second kind:

$$ik_0 R X(\vec{r}) + \frac{\partial}{\partial n} \int_M X(\vec{r}') \frac{\partial}{\partial n'} G_0(\vec{r}, \vec{r}') d\vec{r}' = -\frac{\partial H^{\text{in}}(\vec{r})}{\partial n}, \quad (16)$$

where $G_0 = i/4H_0^{(1)}(k|\vec{r} - \vec{r}'|)$ is the 2D free-space Green's function ($H_0^{(1)}$ stands for the Hankel function), and $X = H^+ - H^-$ is the unknown surface-current density.

Note that in Eq. (14) and hence in IE (16), the term containing the product $k_0 R$ is a simple perturbation to the PEC boundary condition and the IE, respectively. That is why analytical regularization of IE (16) can be done in the same way as for a PEC screen, and a smooth passing to the limits $k_0 \rightarrow 0$ and $R \rightarrow 0$ is possible at every step of this procedure. The inversion of the static part of IE (16) is based on the diagonalization of the integral operator with a hyper-type singularity. This is due to the existence of a set of orthogonal eigenfunctions of the IE static limit: for example, if M is a straight interval, i.e., if the strip is flat, they are the weighted Chebyshev polynomials. Further details of this analysis can be found in [15, 16], for a circularly curved resistive strip and for a flat resistive strip, respectively. In the alternative case of the E-polarization, the role of potential function is played by the electric-field component parallel to the strip generatrix, $E = E_z$. Then the resistive boundary conditions (1), (2) take the form as

$$\frac{1}{2} \left(\frac{\partial E^+}{\partial n} - \frac{\partial E^-}{\partial n} \right) + \frac{ik_0}{Z_0 R} (E^+ + E^-) = 0, \quad (17)$$

$$E^+ - E^- = 0. \quad (18)$$

These conditions, together with the single-layer representation of the scattered field E^{sc} , lead us to the following IE of the second kind:

$$Y(\vec{r}) + \frac{ik_0}{R} \int_M Y(\vec{r}') G_0(\vec{r}, \vec{r}') d\vec{r}' = -\frac{ik_0}{R} E^{\text{in}}(\vec{r}), \quad (19)$$

where $Y = \partial E^+ / \partial n - \partial E^- / \partial n$ is the unknown surface-current density.

Integral equation (19) has a logarithmic-singular kernel G_0 . Such a singularity is integrable, hence this IE is of the Fredholm second-kind provided that $R \neq 0$. That is why it can be discretized by using any usual discretization scheme with local or global-basis expansion functions. One can see that the norm of this IE operator is finite for any $R \neq 0$ and proportional to k_0 . Therefore, it may be stated that IE (19) is based on the analytical inversion of the static limit of the full-wave scattering problem. However, unlike in the H-case, the limit forms of (17), (19) for $k_0 \rightarrow 0$ and $R \rightarrow 0$ are essentially different. For any $R \neq 0$ the static limit of (17) is not the PEC condition; besides, the static limit of the solution to IE (19) is identical zero. Still besides, one can see that if R is purely imaginary or purely real, the ratio $ik_0^{-1} R$ plays the role of a Lavrentyev or a Bakushinsky regularization parameter, respectively [17, 18].

In the case of a circularly curved open resistive strip of radius a (Fig. 1), IEs (16) and (19) can be transformed with discrete Fourier transform, and further static-part inversion can be done in the transform domain [15]. The radar cross-sections of such a strip illuminated by a plane wave are presented in Figs. 2 and 3. In the flat-strip case, IEs can be transformed into the integral Fourier transform domain. Static part inversion can be done in the latter

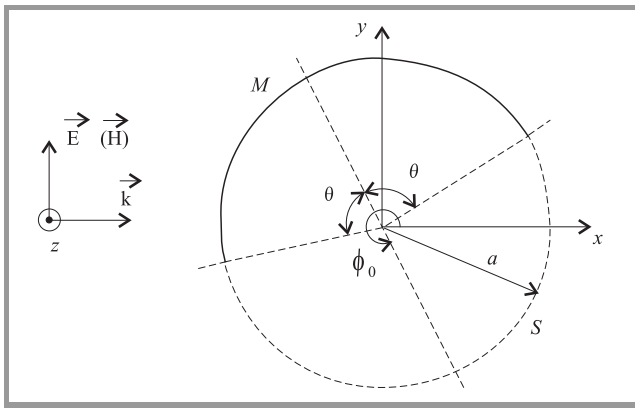


Fig. 1. Scattering geometry of the cross-section of a circularly curved resistive strip.

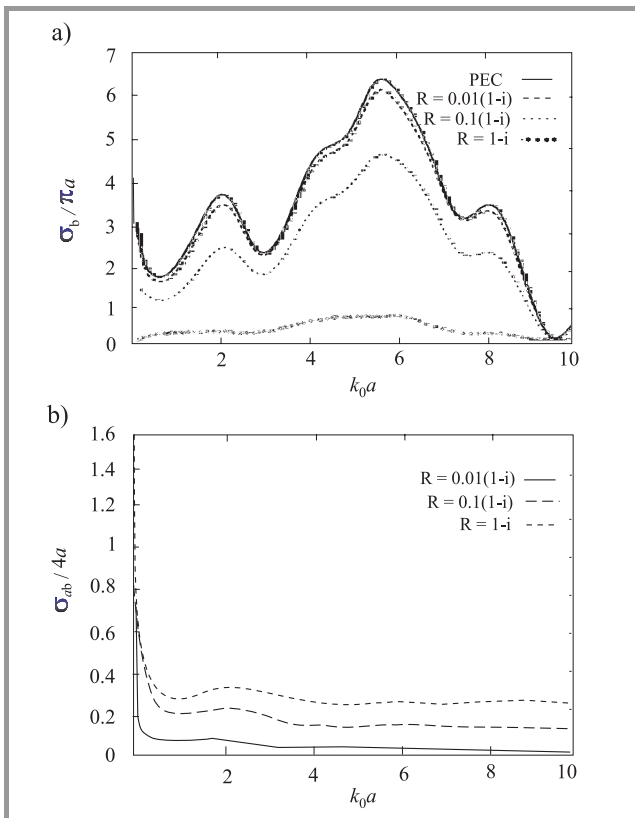


Fig. 2. Lossy resistive strip characteristics in the E-polarization: (a) normalized backward (radar) scattering cross-sections, and (b) absorption cross-sections as functions of the normalized frequency k_0a . $\phi_0 = 170^\circ$, $\theta = 90^\circ$.

domain as well, (see [16]), with the Bessel functions (transformed Chebyshev polynomials) as a basis. The algorithms based on the space-domain and transform-domain MAR are equally high-efficient. A final remark can be done about the extension of MAR solution to a strip with the resistivity varying along the contour M . In this case, R in IEs (16) and (19) must be viewed as a function of \vec{r} . This circumstance does not change the basic properties of IEs, and hence the same MAR schemes work out, although the

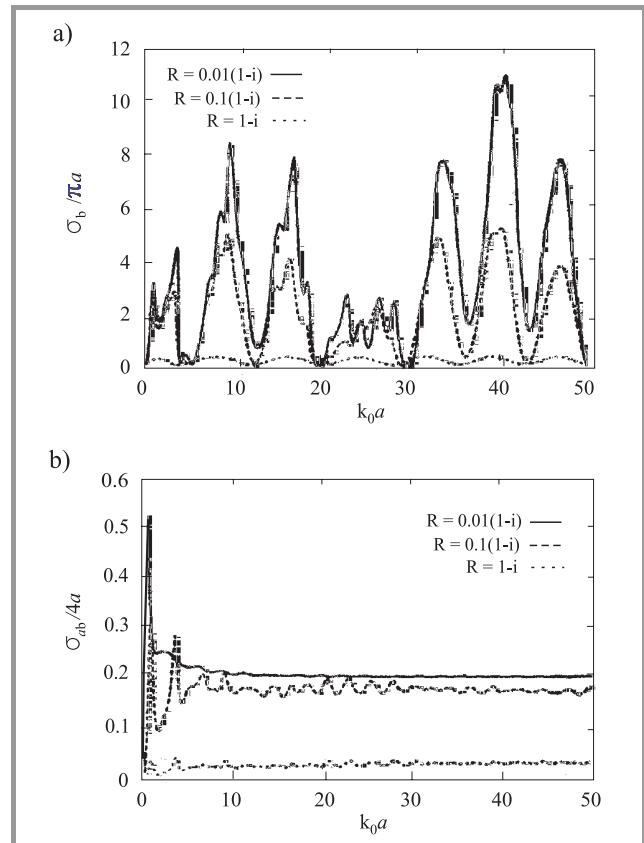


Fig. 3. Lossy resistive strip characteristics in the H-polarization: (a) normalized backward (radar) scattering cross-sections, and (b) absorption cross-sections as functions of the normalized frequency k_0a . $\phi_0 = 170^\circ$, $\theta = 90^\circ$.

rate of convergence gets worse. Based on such a modified algorithm, a cylindrical reflector antenna with a variable-resistivity edge loading was analyzed in [19].

4. Material and impedance strip scattering

In the homogeneous material-strip scattering, we start from the boundary conditions (3), (4). Together with the representation of the scattered field as a sum of a single- and a double-layer potentials, they yield now not one but two second-kind decoupled IEs. Each of the latter can be further treated in the same way as it was done previously for a resistive strip scattering with a H-wave and an E-wave incident, respectively. Paper [20] dealt with solving these equations after converting them to the integral Fourier-transform domain. In the E-polarization case, material thin-strip boundary conditions lead us to a similar pair of the second-kind decoupled IEs, with the parameters R and S interchanged. Hence, in the material-strip scattering, a difference in the electromagnetic behavior between the E-wave and H-wave cases vanishes. Note that, to build the scattered field, the contributions from the solutions of the both IEs

must be taken into account. In the scattering by a multilayer material strip or an impedance strip, the boundary conditions (5), (6) or, equivalently, Eqs. (11) should be used. They bring us to the pair of coupled IEs of the second kind, where cross-resistivity W plays the role of the coupling parameter. If the surface impedances are the same: $Z^+ = Z^-$, then $R = \frac{1}{2}Z^+$, $S = (2Z^+)^{-1}$, $W = 0$, and hence the IEs again decouple. Special case of $Z^+ = -Z^-$ can be considered as well [4].

5. Imperfect strip grating scattering

In the case of the scattering of plane waves by a flat grating made of identic periodically spaced resistive, material or impedance strips of period l (Fig. 4), the same MAR approach as for a single strip can be used. This is due to the fact that in the kernels of corresponding IEs, the quasi-periodic free-space Green's function, G_p , takes the place of G_0 . As $G_p = G_0 + P$, where P is a regular function at $\vec{r} \rightarrow \vec{r}'$, the singularities are kept the same, and hence a similar static-part inversion results in the regularized infinite-matrix equations. A grating of flat resistive

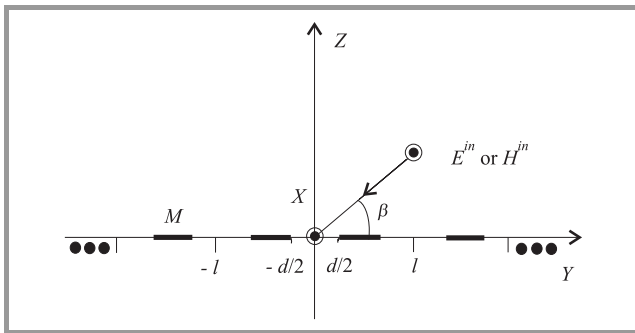


Fig. 4. Scattering geometry of the cross-section of a flat resistive-strip or dielectric-strip grating.

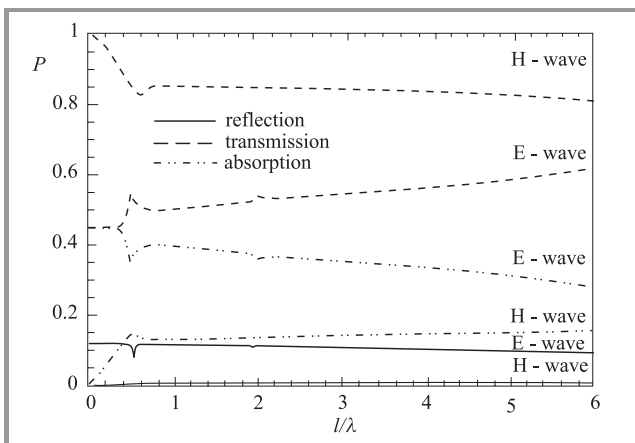


Fig. 5. Transmitted, reflected and absorbed power fractions for the scattering by a resistive-strip grating as functions of the normalized frequency l/λ ($k_0 = 2\pi/\lambda$). $\beta = 30^\circ$, $d/l = 0.5$, $R = 1$.

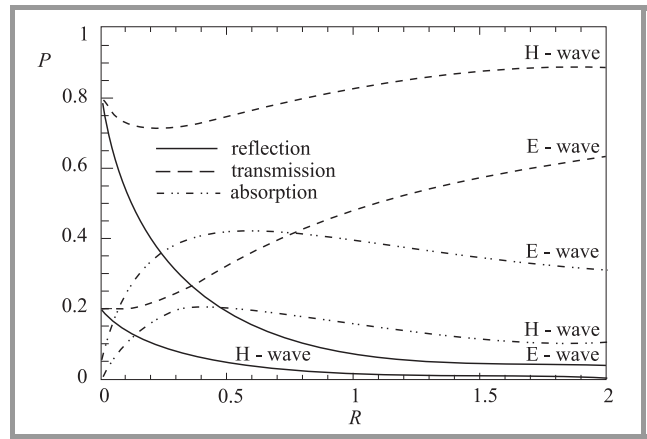


Fig. 6. Power fractions for the scattering by a resistive-strip grating as functions of the normalized resistivity. $\beta = 30^\circ$, $l/\lambda = 0.5$, $d/l = 0.5$.

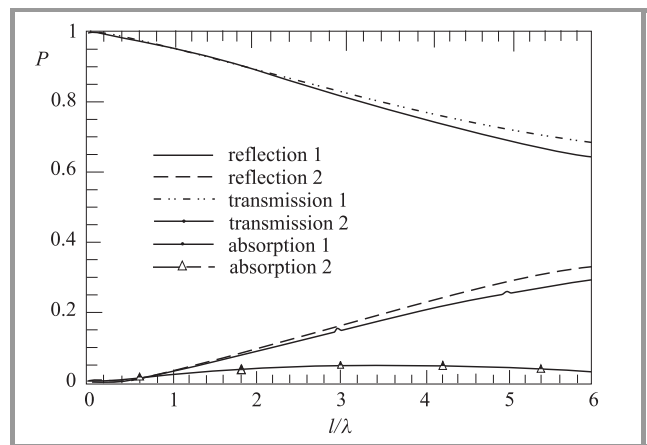


Fig. 7. Transmitted, reflected and absorbed power fractions for the H-wave scattering by a dielectric-strip grating as functions of the normalized frequency for $\beta = 90^\circ$, $d/l = 0.5$, $b/l = 0.01$, $\epsilon_r = 10 + i$, $\mu_r = 1$. Two models are compared: 1 – high-contrast, i.e. R and S based on Eq. (8), and 2 – low-contrast, i.e. R based on Eq. (7) and $S = i\infty$.

strips has been considered in [10, 21 – 24]. Note that in the H-wave case, the results published in [21] were erroneous as the matrix elements did not decrease with greater indices. This is because no regularization of a hyper-singular IE was performed. The latter was developed in [22, 23], where it was noted that the same mistake was characteristic for the other papers considering the scattering of H-waves by a resistive strip grating. In the E-wave case, the results published in [10, 21] are correct and agree with the data of [22 – 24] where different discretizations were used. In Figs. 5 and 6, the power fractions (normalized powers of transmission, reflection and absorption) in the plane wave scattering by a resistive strip grating are presented [22]. In Figs. 7 and 8, the same is presented for the scattering by a thin-strip dielectric grating, which was also considered in [22]. Note that the latter results were confronted with the exact solution of the Fredholm second-kind

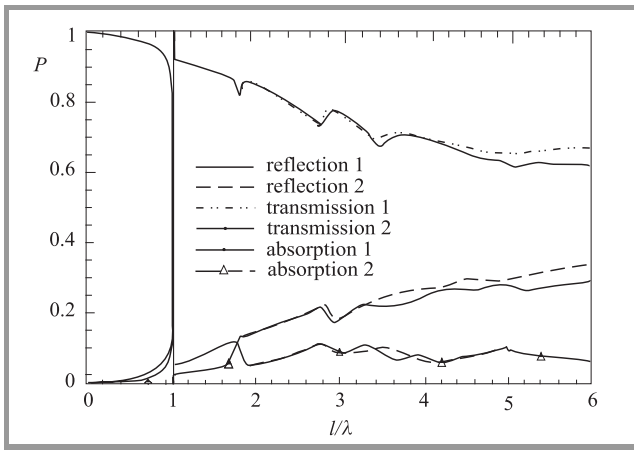


Fig. 8. Transmitted, reflected and absorbed power fractions for the E-wave scattering by a dielectric-strip grating as functions of the normalized frequency for $\beta = 90^\circ$, $d/l = 0.5$, $b/l = 0.01$, $\epsilon_r = 10 + i$, $\mu_r = 1$. Two models are compared: 1 – high-contrast, i.e. R and S based on Eq. (8), and 2 – low-contrast, i.e. R based on Eq. (7) and $S = i\infty$.

“domain” IE for a finite-thickness dielectric strip grating. Comparison showed a very good agreement for the strip thickness being $1/10$ of the period. The scattering by an impedance strip grating has not been analyzed with MAR so far.

6. Imperfect disk scattering

Consider a curved rotationally symmetric disk supporting resistive boundary conditions (1), (2). Here, two simplest diffraction problems arise: excitation of the disk by either a coaxial vertical electric dipole (CVED) or a magnetic one (CVMD). Figure 9 demonstrates an example of such a scattering geometry associated with a flat disk of radius a placed on top of a dielectric substrate. The field in such a geometry is ϕ -independent and can be expressed via a single potential function: H_ϕ or E_ϕ , respectively [25]. In the case of electric (or magnetic) dipole, we arrive at the singular IE of the second kind similar to IE (16) (or (19)),

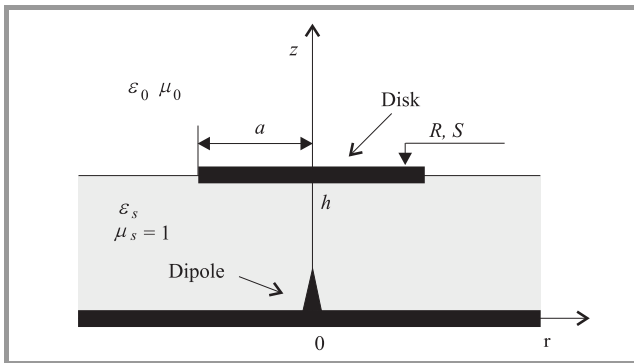


Fig. 9. Scattering geometry of the cross-section of a circular disk on a grounded dielectric substrate.

with the ϕ -independent scalar 3D Green’s function K_0 taking place of G_0 :

$$K_0(\vec{r}, \vec{r}') = r' \int_0^{2\pi} \frac{e^{ik_0\rho}}{\rho} \cos\psi d\psi, \quad (20)$$

where

$$\psi = \phi - \phi', \quad \rho = [r^2 + r'^2 + 2rr' \cos\psi + (z - z')^2]^{1/2}. \quad (21)$$

The domain of integration in IE correspondingly changes to an open curve in the halfplane ($r \geq 0, z$). Note that the function K_0 has the same logarithmic singularity as G_0 , if $\vec{r} = (r, z) \rightarrow \vec{r}'$ [25, p. 67]. In the CVED-case, regularization is needed to reduce the problem of the disk scattering to the infinite-matrix equation of the Fredholm second-kind. This is done by applying a Galerkin scheme with the special Jacobi polynomials, which form the set of orthogonal eigenfunctions of IE static limit. In the CVMD-case, the basic IE is immediately of the Fredholm second kind provided that $R \neq 0$, and may be discretized via any reasonable projection scheme. In Figs. 10 to 12, the frequency scans of the power fractions related to the CVED-excited resistive flat-disk antenna on top of a grounded dielectric substrate are presented [26]. All the power values are normalized to

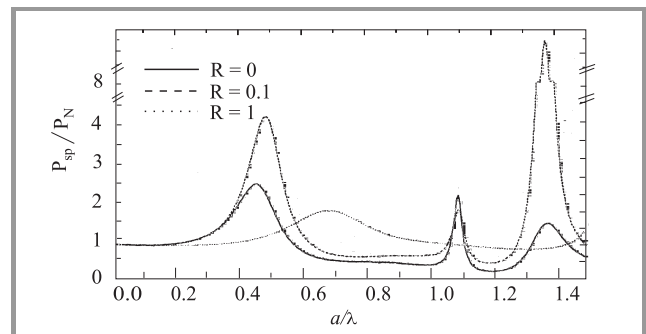


Fig. 10. Normalized radiated power as a function of the normalized frequency a/λ , for a VED-excited resistive circular-disk on a substrate. $\epsilon_s = 1.07$, $h/a = 0.5$, and R as indicated.

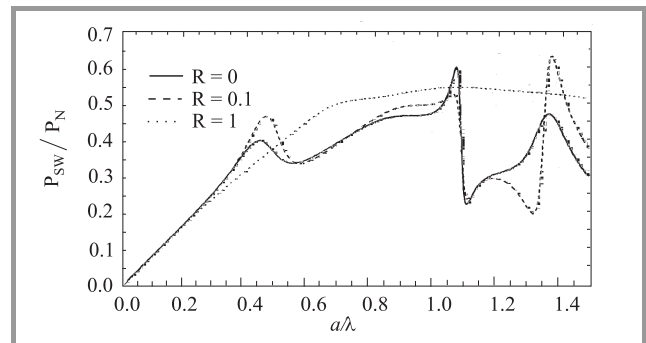


Fig. 11. Normalized surface-wave power as a function of the normalized frequency a/λ , for a VED-excited resistive circular-disk on a substrate. $\epsilon_s = 1.07$, $h/a = 0.5$, and R as indicated.

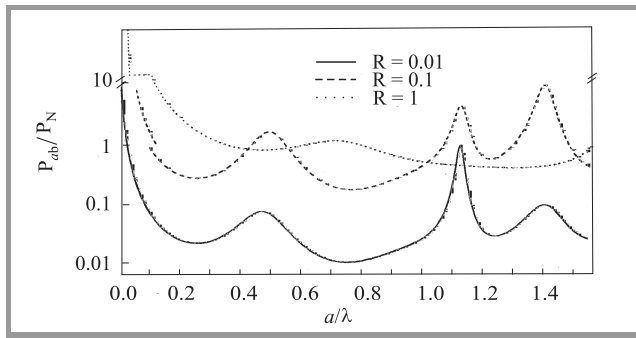


Fig. 12. Normalized absorbed power as a function of the normalized frequency a/λ , for a VED-excited resistive circular-disk on a substrate. $\epsilon_s = 1.07$, $h/a = 0.5$, and R as indicated.

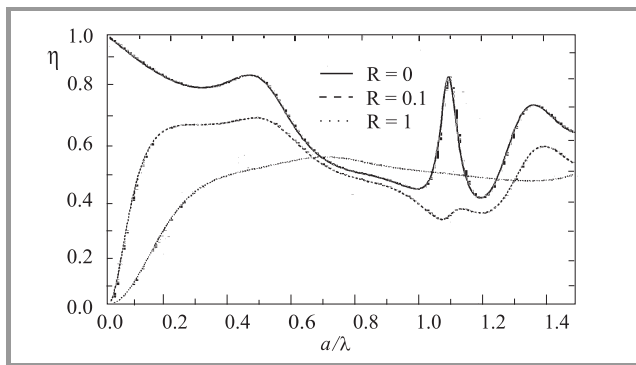


Fig. 13. Radiation efficiency of a VED-excited resistive disk antenna as a function of the normalized frequency.

the power radiated by a VED on a PEC plane. Figure 13 demonstrates the variation of the radiation efficiency in the same frequency band.

In the case of a thin flat material disk of high dielectric and magnetic constants, the boundary conditions (3) and (4) yield a set of two IEs, for the either type of coaxial excitation. Each of them is analogous to one of the resistive-disk IEs, therefore regularization and discretization is done as above. In [27], these IEs have been transformed to the

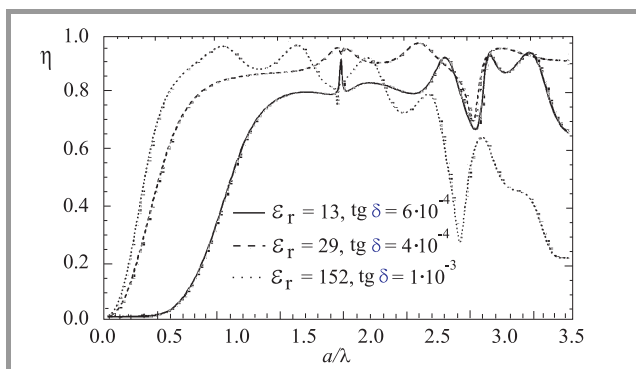


Fig. 14. Radiation efficiency of a thin-dielectric disk antenna as a function of the normalized frequency. $\epsilon_s = 1.07$, $h/a = 0.05$, $b/a = 0.01$, $\mu_r = 1$, and ϵ_r as indicated.

Hankel-transform domain and converted to the dual integral equations for the surface-current transforms. Expansion functions are then transformed to the special-type Bessel functions depending on the type of IE. Numerical solution is very efficient and enables one to minimize the error to machine precision. Figure 14 shows the radiation efficiency of a dielectric disk antenna on a grounded dielectric substrate, fed by a CVED, as a function of the normalized frequency a/λ .

7. Conclusions

It is possible to modify the MAR solutions, previously developed in the PEC-screen scattering, to the imperfect thin screens: resistive, material, and impedance ones. This opens a way for a numerically exact analysis of not only the scattering but also the absorption of waves by the penetrable and impenetrable screens. We presented the illustrations related to the cases of curved strip, flat strip grating, and flat disk on a substrate. Some other results of analysis can be found in [15, 19, 22, 26, 27].

References

- [1] Y. R. Grinberg, "Boundary conditions for electromagnetic field in the presence of thin metallic shells", *Radio Eng. Electron Phys.*, vol. 26, no. 12, 1981 (transl. Engl).
- [2] G. Bouchitte and R. Petit, "On the concepts of a perfectly conducting material and of a perfectly conducting and infinitely thin screen", *Radio Sci.*, vol. 24, no. 1, pp. 13–26, 1989.
- [3] G. Bouchitte, "Analyse limite de la diffraction d'ondes electromagnetiques par une structure mince", *C.R. Acad. Sci. Paris*, vol. 311, Ser. II, pp. 51–56, 1990.
- [4] E. Bleszynski, M. Bleszynski, and T. Jaroszewicz, "Surface-integral equations for electromagnetic scattering from impenetrable and penetrable sheets", *IEEE Anten. Propag. Mag.*, vol. 36, no. 6, pp. 14–25, 1993.
- [5] T. B. A. Senior and J. Volakis, *Approximate Boundary Conditions in Electromagnetics*. London: IEE Press, 1995.
- [6] D. J. Hoppe and Y. Rahmat-Samii, *Impedance Boundary Conditions in Electromagnetics*. Taylor and Francis, 1995.
- [7] T. B. A. Senior, "Diffraction by a semi-infinite metallic sheet", *Proc. Royal Soc. A*, vol. 213, pp. 436–458, 1952.
- [8] R. F. Harrington and J. R. Mautz, "An impedance sheet approximation for thin dielectric shells", *IEEE Anten. Propag.*, vol. AP-23, no. 4, pp. 531–534, 1975.
- [9] T. B. A. Senior, "Backscattering from resistive strips", *IEEE Trans. Anten. Propag.*, vol. AP-27, no. 6, pp. 808–813, 1979.
- [10] R. C. Hall and R. Mittra, "Scattering from a periodic array of resistive strips", *IEEE Anten. Propag.*, vol. AP-33, no. 9, pp. 1009–1011, 1985.
- [11] T. B. A. Senior and J. L. Volakis, "Sheet simulation of a thin dielectric layer", *Radio Sci.*, vol. 22, no. 7, pp. 1261–1272, 1987.
- [12] T. B. A. Senior, "Generalized boundary and transition conditions and the question of uniqueness", *Radio Sci.*, vol. 27, no. 6, pp. 929–934, 1992.
- [13] Z. T. Nazarchuk, *Singular Integral Equations in Scalar Diffraction Theory*. Lvov: Inst. Physics and Mechanics Press, 1994.

- [14] A. I. Nosich, "Method of analytical regularization in wave scattering and eigenvalue problems: foundations and review of solutions", *IEEE Anten. Propag. Mag.*, vol. 42, no. 3, pp. 34–49, 1999.
- [15] A. I. Nosich, Y. Okuno, and T. Shiraishi, "Scattering and absorption of E- and H-polarized plane waves by a circularly curved resistive strip", *Radio Sci.*, vol. 31, no. 6, pp. 1733–1742, 1996.
- [16] E. I. Veliev, K. Kobayashi, T. Ikiz, and S. Koshikawa, "Analytical-numerical approach for the solution of the diffraction by a resistive strip", in *Proc. Int. Symp. Anten. Propag. (ISAP-96)*, Chiba, 1996, pp. 17–19.
- [17] M. M. Lavrentyev, *Some Ill-Posed Problems of Mathematical Physics*. Novosibirsk: SO AN SSSR Publ., 1962 (in Russian).
- [18] A. B. Bakushinsky, "About one numerical method of solving the Fredholm first-kind integral equations", *USSR J. Comput. Mat. Math. Phys.*, vol. 5, no. 4, pp. 744–749, 1965.
- [19] A. I. Nosich, V. B. Yurchenko, and A. Altıntaş, "Numerically exact analysis of a 2-D variable-resistivity reflector fed by a complex-point source", *IEEE Trans. Anten. Propag.*, vol. AP-45, no. 11, pp. 1592–1601, 1997.
- [20] E. I. Veliev, S. Koshikawa, and K. Kobayashi, "Diffraction of a plane wave by a thin material strip: solution by the analytical-numerical approach", in *Proc. Int. Conf. Math. Meth. EM Theory (MMET'2000)*, Kharkov, 2000, vol. 1, pp. 189–192.
- [21] R. Petit and G. Tayeb, "Theoretical and numerical study of gratings consisting of periodic arrays of thin and lossy strips", *J. Opt. Soc. Am. A*, vol. 7, no. 9, pp. 1686–1692, 1990.
- [22] T. L. Zinenko, A. I. Nosich, and Y. Okuno, "Plane wave scattering and absorption by resistive-strip and dielectric-strip periodic gratings", *IEEE Trans. Anten. Propag.*, vol. AP-46, no. 10, pp. 1498–1505, 1998.
- [23] A. Matsushima, T. L. Zinenko, H. Minami, and Y. Okuno, "Integral equation analysis of plane wave scattering from multilayered resistive strip gratings", *J. Electromagn. Wav. Appl.*, vol. 12, no. 10, pp. 1449–1469, 1998.
- [24] S. L. Prosvirnin, S. A. Masalov, A. V. Ryzhak, and V. M. Shkil, "Electromagnetic wave diffraction by a flat grating of resistive strips", *Radiotekhn. Elektron.*, vol. 43, no. 7, pp. 792–796, 1998 (in Russian).
- [25] V. I. Dmitriev and E. V. Zakharov, *Integral Equations in Electromagnetic Problems*. Moscow: Moscow State University Press, 1987 (in Russian).
- [26] N. Y. Bliznyuk and A. I. Nosich, "Numerical analysis of a lossy circular microstrip antenna", in *Radio Physics and Electronics*. Kharkov: IRE Press, 1999, vol. 4, no. 3, pp. 125–128.
- [27] N. Y. Bliznyuk and A. I. Nosich, "Numerical analysis of a dielectric disk antenna", in *Radio Physics and Electronics*. Kharkov: IRE Press, 2000, vol. 5, no. 1, pp. 49–54 (in Russian).

Alexander I. Nosich was born in 1953 in Kharkov, Ukraine. He had graduated from the Kharkov State University and earned his M.Sc., Ph.D. and D.Sc. (higher doctorate) degrees, all in radio-physics, in 1975, 1979 and 1990, respectively. Since 1979, he is on research staff of IRE NASU as a scientist. In 1992–2000, he held visiting professorships and guest-scientist fellowships in Turkey, Japan, Italy and France. In 1995, he was the organizer and first chairman of the IEEE AP Society East Ukraine Chapter (now joint with MTT, ED, AES, GRS and NPS Societies), the first one in the Former Soviet Union. In 1996–2000, he was the chapter secretary-treasurer. Since 1995, he is on the editorial board of the *Microwave and Optical Technology Letters*. In 1990–2000, he was an organizer and technical program committee co-chairman of the series of international conferences on *Mathematical Methods in Electromagnetic Theory (MMET)* in the USSR and Ukraine. His research interests include wave scattering, radiation, propagation and absorption studied by the analytical regularization techniques, and the history of microwaves.
e-mail: alex@emt.kharkov.ua
Institute of Radiophysics and Electronics
National Academy of Sciences
Ulitsa Proskury 12, Kharkov 61085, Ukraine